

Finite-mass correction to 2D Black-hole evaporation rate

Liora Dori and Amos Ori

Department of Physics

Technion-Israel Institute of Technology

Haifa 3200, Israel

(Dated: July 9, 2012)

Abstract

We numerically analyze the evolution of a two-dimensional dilatonic black hole, within the CGHS model. We focus our attention on the finite-mass corrections to the universal evaporation rate which applies at the large-mass limit. Our numerical results confirm a previous theoretical prediction for the first-order ($\propto 1/M$) correction. In addition, our results strongly suggest that the next-order ($\propto 1/M^2$) term vanishes, and provide a rough estimate for the third-order term.

I. INTRODUCTION

In the semiclassical theory of gravity, macroscopic non-spinning black holes (BHs) emit a thermal radiation corresponding to the Hawking temperature $T_H = \hbar c^3 / (8\pi k_B G M)$ [1]. This amounts to an outflux rate \dot{E} which is strictly proportional to $1/M^2$.

However, this simple and universal result is expected to hold only at the macroscopic limit ($M \rightarrow \infty$), and one may anticipate a finite-mass correction. The origin of this correction may be understood as follows: To derive the quantum outflux one has to analyze the (backward) propagation of the field's modes on the BH background, from future null infinity (FNI) back to past null infinity (PNI). Hawking's original derivation uses the *classical Schwarzschild geometry* as the background metric (over which the field's modes are propagated). This is a reasonable approximation as long as the BH is very massive (compared to the Planck mass M_{Pl}). However, in principle, one should instead use the self-consistent *semi-classical* geometry as the background BH metric. The smaller the BH mass M , the larger is the expected deviation of the semiclassical geometry from the classical Schwarzschild solution. Correspondingly, one should expect a finite-mass correction to the universal Hawking outflux, which grows with decreasing M .

It may be of interest to evaluate this finite-mass correction to the semiclassical outflux. For example, it has been argued [2] (in the framework of two-dimensional gravity) that this correction actually reveals the fundamental non-thermal character of the semiclassical outflux. Such deviations from thermality could be highly relevant to the attempts to estimate the possible amount of correlations between the emitted particles (that is, the amount of “information” encoded in Hawking radiation). However, it is difficult to calculate such finite-mass corrections in the realistic four-dimensional (4D) context. The reason is that there is no known general expression for the renormalized stress-energy tensor $\hat{T}_{\alpha\beta}$ in 4D, which makes it hard to construct the semiclassical BH geometry (over which the quantum field's modes are to be propagated).

The situation is much simpler in the two-dimensional (2D) context, however. Callan, Giddings, Harvey and Strominger (CGHS) [3] introduced a formalism of 2D gravity in which the metric is coupled to a dilaton field ϕ and to a large number N of identical massless scalar fields. In this 2D framework $\hat{T}_{\alpha\beta}$ is known explicitly, allowing one to translate semiclassical dynamics into a closed system of partial differential equations (PDEs) [3]. Although the

exact solution to these PDEs is not known, certain approximate solutions have been derived [4]. Also, it is possible to numerically integrate these PDEs and thereby to explore 2D semiclassical dynamics [2, 5]. Among other things, such a numerical integration allows one to analyze the rate of evaporation for finite BH mass as well.

There is a remarkable difference between 2D and 4D classical BHs: Whereas in the latter the horizon's surface gravity κ scales as $1/M$, in 2D it is *independent of the BH mass*. As a consequence, the (large- M) Hawking temperature is constant (i.e. independent of M) in the 2D framework, and so is the outflux \dot{E} [3]. This contrasts with the 4D case, wherein $\dot{E} \propto M^{-2}$. Though, for the same reasons explained above, this 2D constant outflux only holds in the macroscopic limit, and one should anticipate finite-mass corrections.

In Ref. [4] an approximate solution to the CGHS field equations was constructed, accurate to first order in N/M . Based on this approximate geometry, it is possible to derive [6] the leading-order ($\propto M^{-1}$) finite-mass correction to the 2D constant outflux. The corrected value was found to be $\dot{E} = K[1/4 + c_1 K/M_B + O(M_B^{-2})]$ (in appropriate units; see below). Here $K \equiv N/12$, $c_1 > 0$ is a certain known coefficient [6], and M_B denotes the Bondi mass, which is essentially the remaining BH mass (see section 3 for more details). Note that the outflux increases with time, because M_B steadily decreases.

One of the main goals of this paper is to numerically explore this finite-mass correction to \dot{E} , and to verify the aforementioned $O(1/M_B)$ theoretical prediction.

An independent numerical integration of the CGHS system has been carried out recently by Ashtekar, Pretorius and Ramazanoglu (APR) [2]. They also explored numerically the dependence of the outflux on the BH mass. However, their investigation was restricted to the range of relatively small masses, where the relevant $\propto 1/M_B$ expansion parameter is not quite $\gg 1$ (which makes it harder to interpret \dot{E} in terms of inverse powers of M_B). In the numerical analysis presented here we significantly increase the BH mass, by a factor 2.5. This allows us to carry out a more detailed analysis of \dot{E} in terms of inverse powers of M_B .

When we numerically obtained the (time-dependent) value of \dot{E} , we were struck by its remarkable similarity to the above-mentioned first-order corrected theoretical prediction. In fact, it was not possible to visually distinguish between the numerical and theoretical curves (see Fig. 1 below). This came to us as a surprise, because one may naturally expect to have $O(1/M_B^2)$ corrections as well — and no such corrections can be seen in Fig. 1. This could hint that the coefficient of the $O(1/M_B^2)$ term in the outflux function $\dot{E}(M_B)$ (which has not

yet been derived analytically) may actually vanish. This unexpected observation motivated us to analyze $\dot{E}(M_B)$ in more detail, in order to get a better insight into the $O(1/M_B^2)$ term (and possibly also into the $O(1/M_B^3)$ term).

Our detailed numerical results strongly support the conjecture that the $O(1/M_B^2)$ term indeed vanishes, and also provide a crude estimate of the (non-vanishing) $O(1/M_B^3)$ term.

II. THE MODEL AND FIELD EQUATIONS

The CGHS model [3] consists of a two-dimensional metric $g_{\alpha\beta}$ coupled to a dilaton ϕ and to a large number $N \gg 1$ of identical massless scalar fields f_i . We express the metric in the double-null form, namely $ds^2 = -e^{2\rho}dudv$. The action then reads

$$\frac{1}{\pi} \int dudv \left[e^{-2\phi} (-2\rho_{,uv} + 4\phi_{,u}\phi_{,v} - \lambda^2 e^{2\rho}) - \frac{1}{2} \sum_{i=1}^N f_{i,u}f_{i,v} + \frac{N}{12} \rho_{,u}\rho_{,v} \right]. \quad (2.1)$$

The last term in the action expresses the semiclassical effects, derived from the trace anomaly.

The model also contains a cosmological constant λ^2 . Throughout this paper we set $\lambda = 1$. This choice (along with $\hbar = G = 1$) fully determines the system of units, making all variables dimensionless¹.

To simplify the field equations we introduce new variables (following Refs. [4, 7]): $R \equiv e^{-2\phi}$ and $S \equiv 2(\rho - \phi)$. In these variables the model's evolution equations take the form

$$\begin{aligned} R_{,uv} &= -e^S - K\rho_{,uv}, \\ S_{,uv} &= K\rho_{,uv}/R, \end{aligned} \quad (2.2)$$

where $K \equiv N/12$ [and $\rho = (S - \ln R)/2$ is to be substituted]. There are also two constraint equations:

$$R_{,ww} - R_{,w} S_{,w} + \hat{T}_{ww} = 0, \quad (2.3)$$

where hereafter w stands for either u or v , and \hat{T}_{ww} is the (ww) component of the renormalized stress-energy tensor $\hat{T}_{\alpha\beta}$. From the trace anomaly one obtains [3] (via energy-momentum

¹ Formally it is equivalent to the change of variable $\rho' = \rho + \ln(\lambda)$, which does not affect the field equations otherwise. Note that hereafter we also set $f_i = 0$ in the field equations, as we are dealing here with the evaporation of the BH rather than its formation.

conservation) an explicit expression for \hat{T}_{ww} :

$$\hat{T}_{ww} = K [\rho_{,ww} - \rho^2_{,w} + z_w(w)], \quad (2.4)$$

where $z_w(w)$ is a certain boundary function (to be determined from the initial conditions).

Setting $K = 0$, one recovers the classical evolution equations

$$R_{,uv} = -e^S, \quad S_{,uv} = 0, \quad (2.5)$$

and the constraint equations $R_{,ww} = R_{,w} S_{,w}$. This set of equations admits a one-parameter family of classical solutions [up to gauge transformations of the general form $u \rightarrow u'(u)$, $v \rightarrow v'(v)$], which is the two-dimensional analog of the standard Schwarzschild solution. In the so-called *Eddington coordinates* this solution takes the simple form

$$R = M + e^{v-u}, \quad S = v - u, \quad (2.6)$$

where M is a constant. For each $M > 0$ the solution describes a static BH with mass M . Note that in the classical solution

$$\rho(u, v) = -\frac{1}{2} \ln(1 + M e^{u-v}) \quad (\text{classical}). \quad (2.7)$$

This implies asymptotic flatness ($\rho \rightarrow 0$) at both PNI ($u \rightarrow -\infty$) and FNI ($v \rightarrow \infty$). The special case $M = 0$ (also known as the *linear dilaton* solution) describes a flat spacetime, $\rho(u, v) = 0$.

Next we consider the collapse of a thin shell of mass $M > 0$. Following CGHS, we assume that the shell propagates along an ingoing null line, which we set to be $v = 0$. At the classical level the solution is (2.6) at $v > 0$ and flat at $v < 0$.² At the semiclassical level the geometry is still flat at $v < 0$. However at $v > 0$ the classical geometry (2.7) is now replaced by a corresponding solution of the semiclassical field equations (2.2, 2.3). The characteristic initial data for the semiclassical evolution equations may conveniently be prescribed on the collapsing shell and along PNI: These are exactly the same initial data as in the classical collapsing-shell solution [8].

² This flat solution takes the form $R = e^v(M + e^{-u})$, $S = v - u$. [A gauge transformation $u \rightarrow u' = -\ln(M + e^{-u})$ will then bring it to its more standard form $R = e^{v-u'}, S = v - u'$.]

III. OUTFLUX AT FNI

Throughout the rest of the paper we shall use u and v to denote the Eddington-like coordinates for the semiclassical solution at $v > 0$. They are defined by the requirement that the solution takes the asymptotic form (2.6) at both (left) PNI and FNI (and in addition the collapsing shell is located at $v = 0$).

The shell collapse triggers the onset of *Hawking radiation*, namely a nonvanishing energy outflux $T(u) \equiv T_{uu}(u, v \rightarrow \infty)$ at FNI (it is the same quantity that we denoted by \dot{E} throughout the Introduction)³. It may be obtained from Eq. (2.4) by

$$T(u) = \hat{T}_{uu}(u, v \rightarrow \infty) - \hat{T}_{uu}(u, v = 0) \quad (3.1)$$

[a convenient combination which cancels out the boundary function $z_u(u)$], because presumably no outflux crosses the collapsing shell. This expression depends on the actual solution $\rho(u, v)$ at $v \geq 0$ through the RHS of Eq. (2.4).

In the macroscopic limit ($M \rightarrow \infty$), one may substitute the classical geometry (2.7) for $\rho(u, v)$, obtaining the leading-order expression

$$T(u) \approx \frac{K}{4} \left[1 - \frac{1}{(1 + Me^u)^2} \right] \equiv T_{(0)}^{gl} \quad (\text{zero-order; global}). \quad (3.2)$$

We shall denote the term in squared brackets by $F(u)$ for brevity, and refer to it as the *transition function*, describing the onset of Hawking radiation. It starts from zero at early u , and quickly approaches the asymptotic value 1 at large positive u . Thus, the outflux quickly approaches the constant asymptotic value

$$T \approx \frac{K}{4} \equiv T_{(0)}^{late} \quad (\text{zero-order; asymptotic}) \quad (3.3)$$

This zero-order calculation properly describes the outflux at the large- M limit. However, for a finite-mass BH the expression for T is modified because the semiclassical $\rho(u, v)$ differs from the classical solution (2.7). The leading-order semiclassical correction to the classical solution for R and S (and hence for ρ) has been analyzed in Ref. [4]. Based on this, the leading-order correction to the outflux was calculated in [6]. The asymptotic (i.e. late- u)

³ Note that the outflux T is specifically defined here as the (uu) component of $\hat{T}_{\alpha\beta}$ with respect to the *Eddington coordinate* u (i.e. the one for which $2g_{uv} \rightarrow -1$ at FNI).

result was found to be

$$T(u) \simeq \frac{K}{4} \left[1 + \frac{K}{2M_B(u)} \right] \equiv T_{(1)}^{late} \quad (\text{1st-order; asymptotic}) \quad (3.4)$$

where

$$M_B(u) = M - \int_{-\infty}^u T(u') du' \quad (3.5)$$

is the Bondi mass. (Essentially $M_B(u)$ denotes the remaining BH mass as “seen” by a distant observer [9].)

Finally, by combining the asymptotic result (3.4) with the transition function $F(u)$, we arrive at the global, first-order corrected, expression for the outflux:

$$T(u) \simeq \left[1 + \frac{K}{2M_B(u)} \right] T_{(0)}^{gl} \equiv T_{(1)}^{gl} \quad (\text{1st-order; global}) \quad (3.6)$$

We shall shortly verify this approximate expression for $T(u)$ by comparing it to a numerical simulation.

The global expressions $T_{(0)}^{gl}$ and $T_{(1)}^{gl}$ are obviously more effective than their respective late-time counterparts $T_{(0)}^{late}$ and $T_{(1)}^{late}$, as they properly describe the transient stage of the onset of Hawking radiation. It should be pointed out, though, that the simpler, late-time asymptotic expressions $T_{(0)}^{late}$ and $T_{(1)}^{late}$ also have their advantage: They serve as “universal curves” [2] for $T(M_B)$ (at zeroth and 1st-order in K/M_B , respectively), onto which all evolutions with sufficiently large initial mass should converge, regardless of initial conditions.

IV. NUMERICAL RESULTS

We numerically explored the semiclassical 2D spacetime of shell collapse, using a second-order finite-difference code. The initial mass was taken to be $M = 20K$.⁴ (This is to be compared with the initial value $M = 8K$ used by APR [2], and much smaller values $M \lesssim K$ used in earlier analyses [5]). Full details of the analysis will be presented elsewhere [11]. The domain of integration covers the range of u wherein the Bondi mass decreases from its

⁴ The semiclassical CGHS model admits an exact scaling law in which K changes (that is, the number of scalar fields changes), and at the same time the various model’s variables are rescaled by certain powers of K [2, 4]. In particular, the shell’s mass M , the Bondi mass M_B , and the outflux T all scale as K . The functional dependence of T/K on M_B/K is thus invariant to this rescaling. This scaling law allows one to obtain results for all K values from numerical integrations with a single fiducial K value, e.g. $K = 1$.

original value $M_B = 20K$ up to $M_B \approx 15K$ (at larger u — i.e. smaller M_B — numerical errors start to grow exponentially). We calculated $T(u)$ by Eq. (3.1),⁵ and then constructed $M_B(u)$ from it, through Eq. (3.5).

Figure 1 displays the numerically-obtained function $T(u)$, compared with the global first-order theoretical prediction $T_{(1)}^{gl}(u)$. Both functions T and $T_{(1)}^{gl}$ are plotted against the Bondi mass $M_B(u)$. For reference, the simpler (but less precise) approximate expressions $T_{(0)}^{late}$, $T_{(0)}^{gl}$, and $T_{(1)}^{late}$ are also shown. Remarkably, the numerical curve is visually *indistinguishable* from $T_{(1)}^{gl}(u)$, even in the zoomed figure 1b. This observation came to us as a surprise, because it would be just natural to expect corrections to $T_{(1)}^{gl}(M_B)$ of order $O(K/M_B)^2$. The two grey curves in Fig.(1b) represent our original expectation for the typical order of magnitude of such a putative second-order correction term.⁶ The graph shows no signature of such a correction term. In particular Fig. 1b indicates that if such a second-order term at all exists, it must be \ll than its naively-expected order of magnitude.

This observation led us to suspect that perhaps there actually is no second-order finite-mass correction to $T_{(1)}^{gl}$ and $T_{(1)}^{late}$. Furthermore, it provoked the intriguing possibility that perhaps the first-order corrected expression $T_{(1)}^{late}$ is the *exact* expression for the outflux (in the asymptotic late-time limit).

To address these questions, we explored the residual $\Delta T \equiv T - T_{(1)}^{gl}$ with a much higher zoom level. Figure 2 displays ΔT as a function of M_B ⁷. Note the tiny vertical scale $\sim 10^{-6}$. At such a small scale, the truncation error becomes a significant issue. The numerical simulation used a grid step-size of 0.0025 (in both Eddington coordinates u and v). We also carried out simulations with larger step sizes 0.005 and 0.01, and verified second-order convergence (in a certain range of M_B , displayed in Fig. 2). We then used Richardson extrapolation to correct the truncation error in our finest run (step-size 0.0025). It is the corrected residual ΔT which is shown in Fig. 2.⁸

⁵ In practice we have calculated $\hat{T}_{uu}(u)$ along several lines of constant v , at sufficiently large v values which mimic FNI. These different $v = \text{const}$ lines are indistinguishable in the figures below (see also footnote 8).

⁶ The coefficient of this second-order term has not been analytically calculated so far. The gray curves in Fig. 1a represent a fiducial value, obtained by naively extending the (known) zeroth and first-order coefficients to the next order as a geometric progression.

⁷ For the inspected mass-range, $17.3 \leq M_B \leq 18$, $T_{(1)}^{gl}$ has already approached its asymptotic form $T_{(1)}^{late}$. Therefore we can use the residual ΔT defined above to study the next-order correction term for T^{late} .

⁸ Beside the finite step-size (and round-off) there are two other potential sources of errors in our simulations: (i) We start the simulation at a finite $u = u_0$ (rather than at PNI, $u_0 \rightarrow -\infty$); (ii) we compute \hat{T}_{uu} at

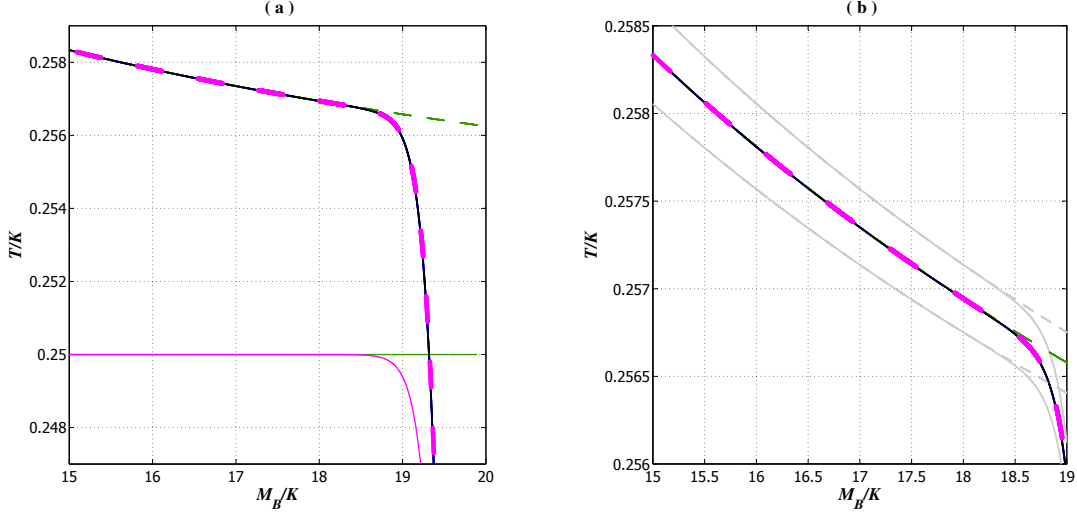


FIG. 1: Comparison of our numerical results for the outflux $T(u)$ (solid black curve), as a function of $M_B(u)$, to certain approximate analytical expressions. (a): The two pink curves represent the (global) zeroth-order and first-order theoretical predictions, $T_{(0)}^{gl}$ (solid) and $T_{(1)}^{gl}$ (dashed). The two green curves represent the corresponding late-time asymptotic expressions $T_{(0)}^{late}$ (solid) and $T_{(1)}^{late}$ (dashed). (b): A blow-up on Fig. 1a. The additional light-gray curves represent one's naive expectation for the typical magnitude of a putative second-order correction term (see main text and footnote therein). Note that the numerical curve is visually indistinguishable from $T_{(1)}^{gl}(u)$, even in the zoom level of Fig. 1b. (The solid black curve actually displays numerical data taken along four different $v = const$ lines throughout the range $24 \leq v \leq 30$, which are again visually indistinguishable.)

Two observations emerge from this figure: First of all, a residual ΔT certainly exists [that is, the first-order corrected expression $T_{(1)}^{late}(M_B)$ is *not* the exact (late-time, asymptotic) expression for T — an issue which was left open in Fig. 1b]. Nevertheless, Fig. 2 is also very suggestive that a second-order correction probably does not exist. The residual ΔT is well matched by a term $-0.05(K/4)(K/M_B)^3 \equiv \Delta T_{(3)}$, though with a relatively large

finite $v = v_{final}$ (rather than at FNI, $v_{final} \rightarrow \infty$). The finite- u_0 error is corrected by the combination of two methods: First, we apply first-order weak-field semiclassical correction to the (otherwise classical) initial data that we set at $u = u_0$ [11]; Second, we run the code with three different u_0 values and perform a Richardson extrapolation. The finite- v_{final} error is handled by trying several different values of $24 \leq v_{final} \leq 32$ and verifying that our results for ΔT are unaffected by further increasing v_{final} .

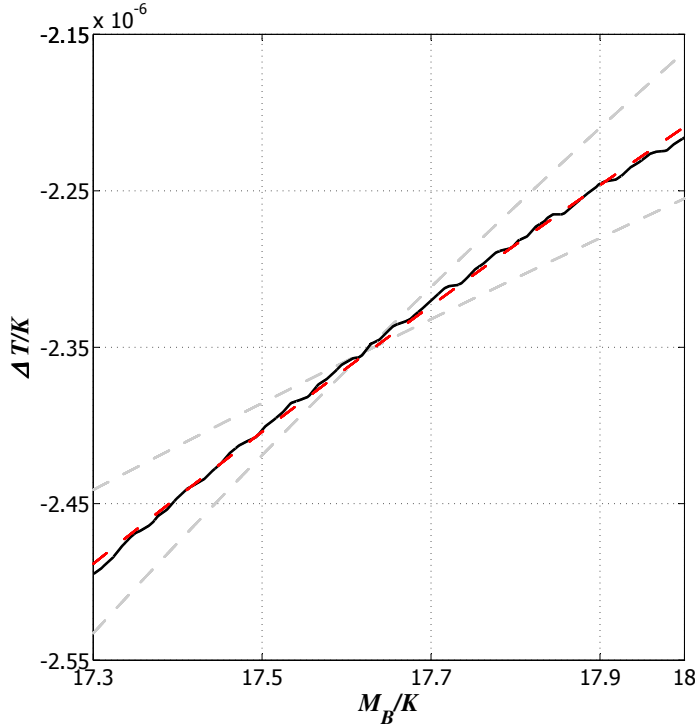


FIG. 2: The residual ΔT (solid black curve) as a function of the Bondi mass M_B . The matched curve $\Delta T_{(3)}$ ($\propto M_B^{-3}$) is shown by dashed red line. For comparison we also display two additional curves (dashed gray) proportional to M_B^{-2} and M_B^{-4} . (The wiggles in the solid numerical curve result from the round-off error.)

numerical uncertainty in the pre-factor, which we estimate as $\sim \pm 25\%$. (This large relative uncertainty is obviously attributed to the tiny overall magnitude of the residual, which is smaller than T by a factor $\sim 10^{-5}$.⁹)

V. SUMMARY

Our numerical results confirm the previous theoretical prediction of the first-order finite-mass correction (3.4,3.6). They further suggest the absence of a second-order correction term, and provide a rough estimate for the third-order term. Our final result is the following

⁹ The main source of this uncertainty is the finite u_0 (see footnote 8). Since we only used three u_0 values, it is hard to assess the effectiveness of the associated Richardson extrapolation.

third-order approximate expression for $T(M_B)$:

$$T_{(3)}^{late} = \frac{K}{4} \left[1 + \frac{K}{2M_B} + c_3 \left(\frac{K}{2M_B} \right)^3 \right] \quad (5.1)$$

along with its global counterpart $T_{(3)}^{gl} = F(u) T_{(3)}^{late}$. Here c_3 is a dimensionless coefficient which we estimate as ~ -0.4 (with about $\sim 25\%$ uncertainty).

It would be desired to find the analogous finite-mass corrections to the Hawking outflux from a 4D semiclassical BH, but this is obviously a much harder task.

Acknowledgment

We would like to thank Abhay Ashtekar, Frans Pretorius, and Fethi Ramazanoglu for helpful discussions. This research was supported by the Israel Science Foundation (grant no. 1346/07)

Note added in Proof: After this work was submitted, Ramazanoglu notified us that he managed to convert the results of Ref. [2] for the mass-dependent outflux, from the modified definitions of outflux and Bondi mass (introduced in Ref. [10]) to the traditional ones [9]. He then carried out an expansion of the (traditional) outflux in inverse powers of (traditional) Bondi mass. His results, truncated after third order, agree with our Eq. (5.1) with $c_3 = -(5/12) \approx -0.42$ [12].

-
- [1] S. W. Hawking, Commun. Math. Phys. **43**, 199 (1975).
 - [2] A. Ashtekar, F. Pretorius and F. M. Ramazanoglu, Phys. Rev. **D83**, 044040 (2011); Phys. Rev. Lett. **106**, 161303 (2011).
 - [3] C. G. Callan, S. B. Giddings, J. A. Harvey and A. Strominger, Phys. Rev. **D45**, R1005 (1992).
 - [4] A. Ori, Phys. Rev. **D82**, 104009 (2010).
 - [5] See also previous numerical works: S.W. Hawking and J.M. Stewart, Nucl. Phys. **B400**, 393 (1993); D. A Lowe, Phys. Rev. **D47**, 2446 (1993); T. Piran and A. Strominger, Phys. Rev. **D48**, 4729 (1993); T. Tada and S. Uehara, Phys. Rev. **D51**, 4259 (1995).
 - [6] A. Ori (Unpublished notes); see <http://physics.technion.ac.il/~amos/outflux.pdf> [see in particular Eq. (141) therein].

- [7] A. Ori, Phys. Rev. **D63**, 104016 (2001).
- [8] This set-up of semiclassical initial data is described in detail in Ref. [4].
- [9] This is the traditional definition of the Bondi mass. In Ref. [10] new definitions were introduced for both the “outflux” and the “Bondi mass”. These new definitions admit some elegant properties. Here we prefer to use the traditional definitions for the outflux and M_B , because these traditional definitions make use only of the local geometric (and dilatonic) behavior at FNI (whereas the definitions introduced in [10] also resort to the time-translation coordinate at left-PNI).
- [10] A. Ashtekar, V. Taveras and M. Varadarajan, Phys. Rev. Lett. **100**, 211302 (2008).
- [11] L. Dori, Ph.D. thesis (in preparation).
- [12] F. M. Ramazanoglu (unpublished notes).